Detection of Spiral Resonator Array for Chipless RFID

Polivka M., Havlíček J., Svanda M., Macháč J.
Department of Electromagnetic Field
Czech Technical University in Prague
Technicka 2, 166 27, Prague 6, Czech Republic
{polivka, havlij18, svandml, machac}@fel.cvut.cz

***Abstract*—Presented paper analyzes the influence of different configurations of the planar resonator arrays of the size 16×4 up to 16×16 elements on the reflection coefficient of the half-wavelength dipole probe in the frequency range 600-1000 MHz. Four different square spiral resonators of the outer diameter 7 mm (~ $0.02\lambda_0$@800 MHz) with various total lengths of the conductor are used as array building elements. It is shown that specific arrangement of the resonators in the array enhances the response of the probe. The work was motivated by the potencial application of such arrays in chipless RFID technology.**

Keywords – chipless RFID, resonator array, spiral resonator

I. INTRODUCTION

Although the RFID technology is known for more than three decades, it started to be used more extensively as far as in the last decade. Today, it is spread in broad fields of applications, such as commercial, industrial, medical, scientific and other areas; basic information can be found e.g. in [1]. One of the most important challenges in RFID technology is the potential replacement of the barcode. Another substantial issue is the production of low-cost TAGs. However as far as the chipless RFID TAGs can offer really low production cost thus the research in this area is very promising. The summary of early works in the field of fully printable chipless RFID transponders can be found e.g. in [2].

The presented paper analyses the influence of several configurations of the planar spiral resonator arrays on the reflection coefficient of a half wavelength dipole probe in the frequency range 600 ÷ 1000 MHz. In this study we focused on the experimental evaluations as the EM analysis based on method of moments (MoM) of the arrays 16×16 elements with proper segmentation is rather time consuming. We discuss the suitable arrangements of planar resonator arrays with a good response for potential application as chipless RFID TAGs.

II. DETECTION OF SPIRAL RESONATOR ARRAYS

A. Spiral resonator elements

The planar square spiral geometry (see Fig. 1) with different total conductor length is used to tune the individual resonators for specific frequency. The outer size of the resonator D_{out} = 7.0 mm is fixed. The width of the strip is w = 0.2 mm, and the spacing between turns is w = 0.2 mm. The parameters of the substrate are ε_r = 3.05, tanδ = 0.003, h = 0.5 mm. We have used 3.3 up to 5 turns to set four resonances with interval of approx. 50 MHz in the frequency range 670-820 MHz, e.g. slightly lower than self-resonance of the dipole probe.

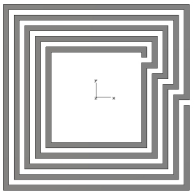

Figure 1. Sketch of the layout of a square spiral resonator.

The self-resonance of the spiral resonator can be calculated from the Thomson's formula $f_0 = 1/2\pi\sqrt{(LC)}$ where the inductance and capacity can be derived according to the relations presented in [3]. Here we have evaluated the resonant frequency from the current phase response, i.e. the change of the orientation of the vector current density evaluated in MoM IE3D simulator.

B. Dipole probe

The symmetrized half-wavelength wire dipole has been used as a probe and placed in different orientation and positions with respect to the array. The length of the dipole was chosen 156 mm, the wire diameter 1 mm, which provides corresponding half-wavelength resonance frequency approx. 910 MHz. The dipole arms were isolated to ensure the same probe-array distance in each measurement. Simple half wavelength loop symmetrization has been used, see Fig. 2.

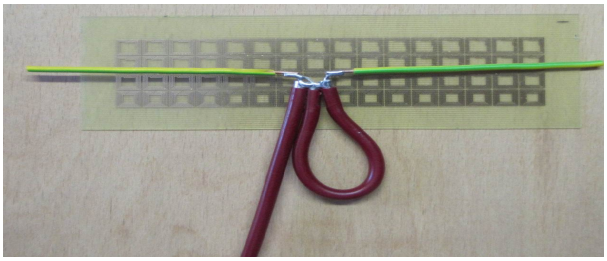

Figure 2. Dipole probe in the vicinity of the resonator array.

B. Influence of the resonator array arrangement on the dipole reflection coefficient

Four types of arrangement of periodical resonator array were manufactured and analyzed. We evaluated the response by means of the deepness of the local minima at the return loss curve representing resonances, e.g. coupling energy of the probe near field to the resonators. The red lines in the array matrix represent the actual probe position at which it has been located to the array. The curves of the return loss graphs corresponding to particular probe positions are distinguished by the color and the number in the legend. The photographs of all array configurations can be seen in particular figures.

Array I consist of 16×4 elements. Each column (with 16 elements) consists of the resonators with the same resonant frequency, see Fig. 3b. Resonators in individual rows (with 4 elements) are situated so that edge position 32 corresponds with the probe enclosed to the column with the highest number of turns (5), i.e. with the minimum resonant frequency approx. 660 MHz. We can see that there are up to four visible element resonances in position No. 32. The lower three ones at approx. 710, 770, and 825 MHz correspond to the resonances of spiral resonators. The highest one, at 910 is the resonance of the probe itself. The lowest resonance of the spiral resonator with the longest conductor is not explicitly visible here as the probe passed probably over of these resonators so that the magnetic flux around the wire is in opposite directions at opposite halves of the resonators.

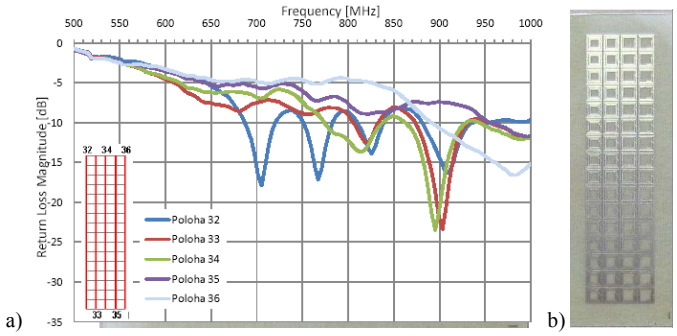

Figure 3. Array I of 16×4 elements a) return loss of the probe, b) photograph of the array

Array II consists of 16×16 elements. The array is formed by 4 arrays as in Array I situated side by side that means each four different resonators are placed next to another, see Fig. 4c. In case the probe is attached vertically, i.e. along the columns with the same type of the resonator the response is weak, see Fig. 4a. While the probe is attached horizontally, i.e. across the rows with different resonators, the response is stronger, see Fig. 4b. The closer is the resonant frequency to the resonant frequency of the probe the deeper is the resonant minimum at the return loss curve. We can notice clear minima for probe edge position No. 22 at frequencies approx. 660, 710, 760, and 820 MHz. The resonance of the probe itself is at frequency 920 MHz. The central position of the probe No. 26 provides clear minima at frequencies approx. 650, 700, 750(760), and 820 MHz. The resonance of the probe is shifted to 890 MHz here. Another phenomenon is the detuning of the probe resonance due to the coupling with individual columns of elements which is here shifted in other probe positions as far as to approx. 880-925 MHz, e.g. 2.2 %.

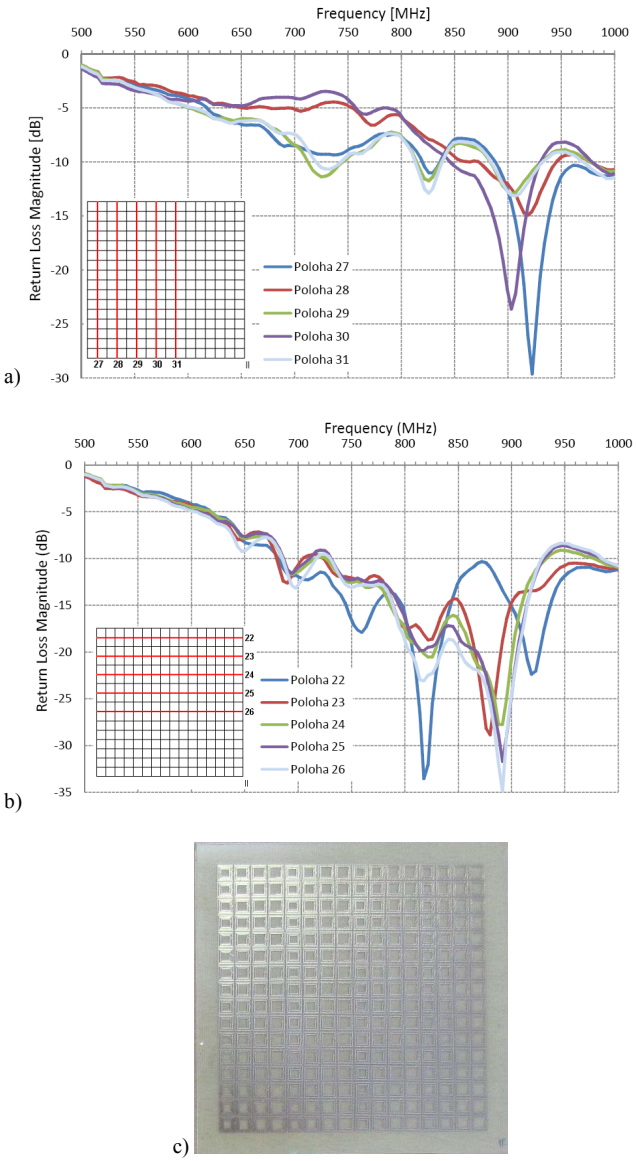

Figure 4. Array II of 16×16 elements, a), b) return loss of the vertical and horizontal probe position, respectively, c) photograph of the array

Array III consists of 16×12 elements. Four sub-arrays with 16×3 elements formed by the resonators with the same resonant frequency are situated side by side. The sub-arrays are sorted in ascending order from the left to the right as resonant frequency increases. So that the lowest resonant frequency sub-array is placed on the left, see Fig. 5b. We can distinguish the strong response of the closest two elements in positions No. 18 (at 680, 720, 770, 840 MHz) while the response of the other two elements is weak, however still distinguishable. The further is the position of the probe to the right the stronger is the response of the elements with higher resonant frequencies.

The resonance of the probe creates loop with two minima at the frequencies 900 (880) and 960 MHz for all of the probe positions here.

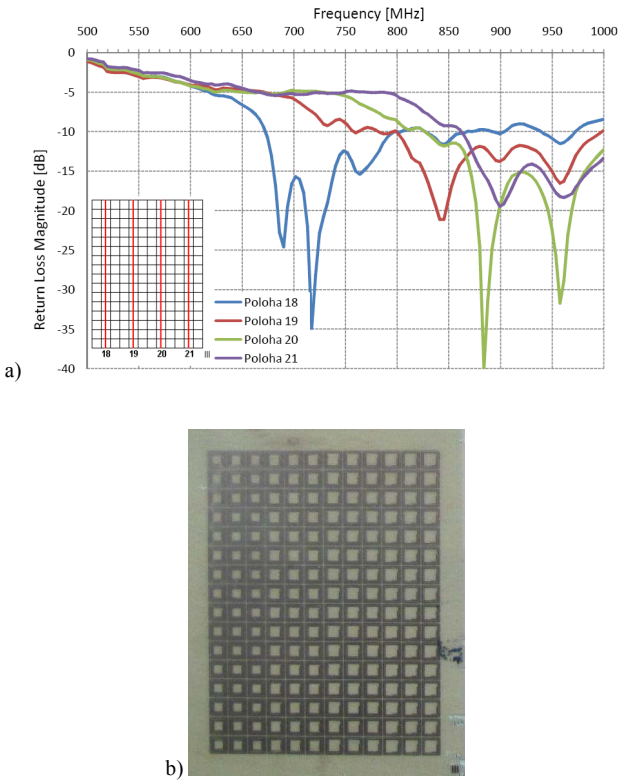

Figure 5. Array III of 16×12 elements, a) return loss of the vertical probe position, respectively, b) photograph of the array

Array IV (denoted in Fig. 6 as IIII) consists of 16×16 elements which are formed by the periodical arrangement of the resonators, whereas the resonator sequence in every next line is shifted by one element. Thus the resonators with the same resonant frequency are placed along the diagonal, see Fig. 6d. The curve No. 14 in Fig. 6a contains 4 minima corresponding to the resonances of all four elements at frequencies: 670, 720, 770, 820 MHz. The resonance at 890 MHz is slightly detuned resonance of the probe. The measurements in positions No. 13 and 15 exhibit nearly the same progression of the reflection coefficient, the third resonance is shifted to approx. 785 MHz and the resonance at 820 MHz is not visible. The curve No. 7 and 9 in Fig. 6b corresponding to the diagonal orientation of the probe contains the minima nearly at the same positions as curve No. 14. The probe resonance is shifted to frequency range 890-920 MHz. In Fig. 6c we can distinguish very strong responses usually at one frequency as the probe is oriented along the opposite diagonal as in case of Fig. 6a. There are the same resonant elements along the probe in the constant distance. For position No. 2 the most significant response is for the lowest resonant elements (660 MHz), while for position No. 3 it is the second lowest resonance (730 MHz).

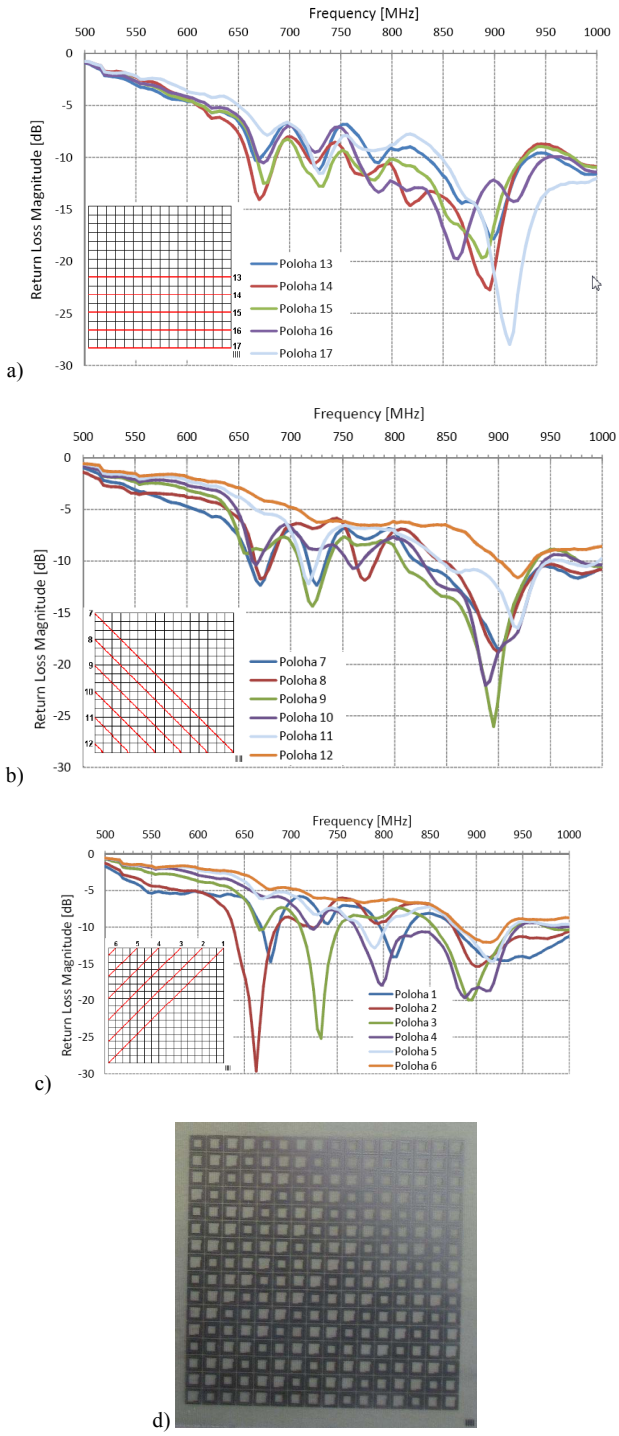

Figure 6. Array IV (IIII) of 16×16 elements, a, b, c) return loss of the horizontal, diagonal across and diagonal along the same resonant frequency elements probe position, respectively, c) photograph of the array

III. DISCUSSION

Detailed discussion of the measured responses shows the strong response exists in the case when elements with different resonant frequency are placed along the probe axis. In such cases, e.g. positions 15, 14, 13, (9, 7), the depth of the local minima is comparable one to another. The closer is the row of the elements with the same resonant frequency to the probe the

stronger is the response and vice versa (26, 22). Further the closer is the probe to the center of the array, e.g. positions 26, 25, the stronger is the response. The close vicinity of the array detunes the self-resonance of the dipole probe from 910 MHz within the frequency range of approx. $880 \div 925$ MHz depending on the position of the probe with respect to the array.

ACKNOWLEDGMENT

This work has been undertaken in the Department of Electromagnetic Field at the Czech Technical University in Prague and was supported under the project SGS10/271/OHK3/3T/13 "Artificial electromagnetic structures for high frequency technology".

REFERENCES

[1] Finkenzeller, K., *RFID Handbook: Fundamentals and Applications in Contactless Smart Cards and Identification*, 2nd edition, John Wiley & Sons, 2005

[2] Preradovic S., Karmakar N.: Advanced Radio Frequency Identification Design and Applications, Fully Printable Chipless RFID Tag (chapter 7), InTech, 2011

[3] Young L., Sobol H.: Advances in Microwaves, *Academic Press*, vol. 8, New York, 1974.